Materials Letters 179 (2016) 146–149

Contents lists available at ScienceDirect

Materials Letters

journal homepage: www.elsevier.com/locate/matlet

Oxygen interstitial mediated effective doping of Al in ZnO:Al films prepared by magnetron sputtering

Shiliu Yin, Jieni Li, Mandar M. Shirolkar, Ming Li, Haiqian Wang *

Hefei National Laboratory for Physical Sciences at the Microscale, University of Science and Technology of China, Hefei, Anhui 230026, People's Republic of China

ARTICLE INFO

Article history:
Received 9 April 2016
Received in revised form
11 May 2016
Accepted 11 May 2016
Available online 16 May 2016

Keywords:
Thin films
Sputtering
Oxygen interstitials
Hydrogen annealing
Doping efficiency

ABSTRACT

How to increase the doping efficiency in ZnO:Al (AZO) films is a longstanding question and a hard nut to crack. In the present work, we report an oxygen interstitial mediated doping effect for AZO films prepared by magnetron sputtering. The concentration of oxygen interstitials (O_i) in the as-grown films is tailored by changing the oxygen partial pressure during sputtering. Although the Al donors are temporarily passivated by O_i, they are easily reactivated through the removal of O_i by post-annealing in hydrogen at 500 °C. Our results show that the as-grown film which has the highest O_i concentration turns out to have the highest carrier concentration after hydrogen annealing, and the doping efficiency is increased by ~10% because of the oxygen interstitial mediated doping effect. We infer that although O_i deactivate Al donors in the as-grown films, they favor the distribution of the doped Al at the atomic level and the formation of Al substituting at Zn sites (Al_{Zn}), and thus, increase the effective Al donors after hydrogen annealing.

1. Introduction

III-group element (Al, Ga, In) doped ZnO is a widely investigated n-type transparent semiconductor with low resistivity [1]. Recently it was shown that doped ZnO may be also very promising for the photo-induced nonlinear optical effects [2]. Because of the fascinating features of ZnO:Al (AZO) films, including high stability in hydrogen plasma and eco-friendly, they are highly expected to replace In_2O_3:Sn (ITO) in various applications as transparent conductive oxide (TCO) films [3,4]. In AZO films, Al acts as the predominant donor. However, the doping efficiency is limited [5–7].

For heavily doped AZO films, most of the doped Al atoms tend to exist in neutral forms, e.g. aggregated Al_2O_3 [5]. Even if Al atoms enter ZnO lattice and substitute Zn (Al_{Zn}), they may still be compensated by the electron acceptors like oxygen interstitials (O_i) [8]. As a result, improving the spatial distribution of Al atoms in the lattice and activating the passivated Al_{Zn} could be a solution to increase the doping efficiency in AZO films [9]. It has been theoretically proven that Al_{Zn} can form complex defects with O_i in the lattice with a low binding energy [10]. On the other hand, hydrogen annealing is an effective method to remove O_i [11,12] resulting in the reactivation of Al_{Zn} donors [13]. Therefore, it should be possible to first increase the distribution of Al in the lattice through introducing O_i, and then increase the doping efficiency by post-annealing in hydrogen. In the present work, we report an O_i-mediated doping effect of Al in sputtering deposited AZO films, and ~10% increase in the Al doping efficiency is achieved.

2. Experiment

AZO films were deposited on BK7 substrates (SIGMA KOKI, Co., Ltd.) by magnetron sputtering (RAS-1100C, SHINCRON Co., Ltd.) with dual ZnO:Al_2O_3 ceramic targets (2.2 wt% Al_2O_3, purity ≈ 99.9%). The chamber pressure was first pumped down to 1×10^{-4} Pa and then Ar (purity ≈ 99.999%)+ O_2 (purity ≈ 99.999%) mixed gas was introduced as sputtering gas to maintain a total working pressure of 0.24 Pa. The ratio of oxygen partial pressure to the total working pressure (R_O) was changed in the range from 0 to ~22 vol%. The substrates were rotated at a constant speed of 100 r/min and not intentionally heated during sputtering. The power density on the targets was 6.2 W/cm^2 and the deposition time was fixed at 1005 s The film thickness was within ~430–575 nm, which was determined by the envelop method from the transmittance spectra [11]. Other deposition details can be found elsewhere [11,14,15]. The as-grown films (25×30 mm^2 in area) were then put into a $\phi 30 \times 400$ mm quartz tube and annealed under pure H_2 atmosphere with a fixed flux of 10 sccm (standard cubic centimeter per minute) at 500 °C. The

* Corresponding author.
E-mail address: hqwang@ustc.edu.cn (H. Wang).

http://dx.doi.org/10.1016/j.matlet.2016.05.072
0167-577X/

heating rate was set to be 5 °C/min. After holding for 30 min, annealed films were then naturally cooled down to room temperature for further measurements.

The microstructural morphologies of AZO films were investigated by field emission-scanning electron microscopy (FE-SEM, JSM-6700 F, JOEL, Ltd., Japan) in plan-view geometry. X-ray diffraction (XRD) patterns were recorded using an X'pert diffractometer (PANalytical B.V.) in θ–2θ geometry at Cu-Kα radiation (λ=1.5418 Å). Raman spectra measurements was performed by LabRam HR (HORIBA, Ltd) at an excitation wavelength of 514.5 nm with a spectral resolution of 0.6 cm^{-1}. Specular transmittance and reflectance in the UV–vis range were measured by a UV–vis–IR4100 spectrophotometer (HITACHI, Ltd., Japan) with a wavelength accuracy of 0.2 nm. The compositional analysis was performed by an inductive coupled plasma–atomic emission spectrometer (ICP-AES, Optima 7300 DV, PerkinElmer, Inc., USA). Van der Pauw method was applied to measure the resistivity. The samples were cut into 10×10 mm^2 squares with silver paste at four corners for Ohmic contact. Hall measurement was performed under a magnetic field of 4630G at room temperature. Both the carrier concentration and mobility were measured three times for each film. The error was within ~2%.

3. Results and discussion

Fig. 1 shows XRD patterns of all the samples and corresponding c-axis lattice spacing results. All samples show a unique (002) diffraction peak of the hexagonal wurtzite structure of ZnO (JCPDS PDF#65-3411), indicating that well crystallized AZO films with c-axis perpendicular to the substrate are obtained [16]. With the increase of R_O, the (002) lattice spacing of the as-grown films increases (black line in Fig. 1b), which can be mainly assigned to the increase of O_i because higher R_O increases the concentration of oxygen in the plasma [11]. Rahmane et al. also reported that for AZO films deposited at higher oxygen content, the c-axis lattice spacing becomes wider [17]. Our results show that the concentration of O_i in the as-grown films can be adjusted by changing R_O.

After hydrogen annealing, the lattice spacing of all the as-grown films decreases, which is mainly due to the removal of O_i by hydrogen [13]. Chang et al. also reported the lattice spacing of AZO films decreases after hydrogen annealing at 500 °C [18]. In addition, the film deposited at higher R_O shows a larger decrease in the lattice spacing after annealing, again implying that more O_i are formed in the as-grown film deposited at higher R_O. This phenomenon also indicates that hydrogen annealing effectively removes O_i, whatever the concentration of O_i is in the as-grown films.

Based on our surface SEM observations (Fig. S1), both R_O and hydrogen annealing have little effect on the surface morphology of the films. Besides, our ICP analysis shows that the Al content in all the as-grown and annealed films is $\sim 2.4 \pm 0.3$ at% (Al/[Al+Zn]), indicating that the composition of the films is neither affected by R_O nor hydrogen annealing.

Fig. 2 shows the Raman spectra of some representative samples. All the as-grown samples show the most intense band centered at ~ 568 cm^{-1} which belongs to the vibration mode of longitudinal optical phonons (LO), a weak band centered at 437 cm^{-1} which belongs to the E_2 transverse mode (TO) and a weak band centered at 516 cm^{-1} which is an additional vibration mode (AM) [19]. The LO mode is mainly caused by the oxygen vacancies (V_O) [20,21], and the AM is attributed to the oxygen at grain boundaries (O_{GB}) which leads to the formation of the built-in electric field near the depletion region around the grain boundaries [22]. As R_O increases, both the LO and AM modes are weakened, indicating the decreased V_O concentration and weakened built-in electric field. The decreased V_O is because of the higher oxygen concentration in plasma at higher R_O. The O_{GB} is mainly affected by the grain size and our surface SEM results have shown that the morphology is nearly the same for all the as-grown films. Thus the weakening of AM should be attributed to the expansion of the depletion region into the grains resulted from the severer passivation of Al_{Zn} donors by the increased O_i at higher R_O [19]. After hydrogen annealing, the LO modes all diminish which is due to the occupation of the V_O sites by hydrogen [23] and the AM is largely weakened which is attributed to the removal of O_{GB} by annealing [11].

Fig. 3 shows the optical band gap values of all the samples obtained from the transmittance (Fig. S2) and reflectance spectra by the Tauc's relation [24]. For the as-grown films, the optical band gap decreases with the increase of R_O. As a result of Moss-Burstein effect [25], the optical band gap value is a direct indication of the carrier concentration. As discussed above, higher R_O leads to increased O_i which passivate Al donors, thus the optical band gap decrease down to ~3.35 eV. Dong et al. also reported that the optical band gap of AZO films prepared by pulsed laser deposition decreases with the increase of oxygen partial pressure [26], which is consistent with our results.

After hydrogen annealing, the optical band gaps are all greatly enlarged, which is because of the effective removal of O_i and reactivation of Al donors. What is more, the optical band gap value shows an increasing trend with the increase of R_O after annealing, indicating a higher concentration of activated Al in films deposited

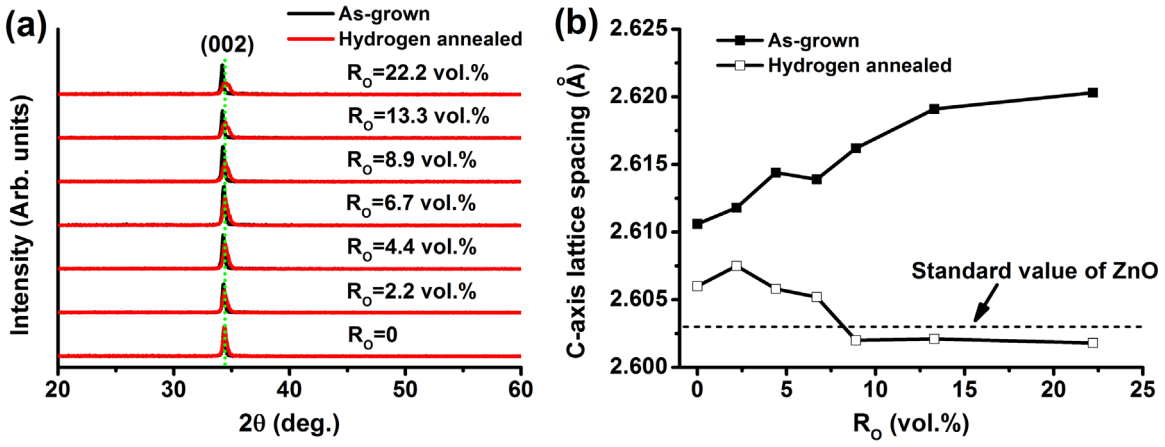

Fig. 1. (a) XRD patterns of all the samples. The dotted line marks the standard (002) diffraction peak of ZnO. (b) Corresponding c-axis lattice spacing results.